Metabolic Pathways Affected in Barth Syndrome

Zaza Khuchua, Yan Huang, Corey Powers, Arnold Strauss.

Cincinnati Children's Research Foundation and University of Cincinnati.

Introduction

Cardiolipin (CL) is a negatively charged mitochondrial phospholipid, which is essential for the assembly and optimal function of many mitochondrial enzymatic complexes, including the electron transport chain. Cardiolipin deficiency in humans results in a multisystem pediatric disorder, Barth syndrome (BTHS), and is caused by mutations in the tafazzin (*Taz*) gene. Barth syndrome patients and tafazzin-deficient mice have abnormal cardiolipin composition in mitochondria and develop dilated cardiomyopathy.

Tafazzin knockdown (Taz-KD) and cardiolipin deficiency in our mouse model of BTHS result in a two-fold reduction of mitochondrial oxygen consumption in cardiomyocytes and impaired activity of mitochondrial complex III (cytochrome bc1 complex) (Figure 1).

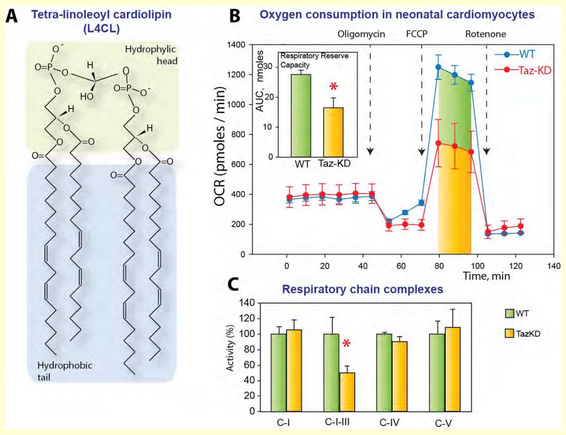

Figure 1. *Tetralinoleoyl cardiolipin (L4CL) is the predominant cardiolipin in cardiac mitochondria (**A**). Impaired cellular O_2 consumption (**B**) and complex III deficiency (**C**) in L4CL-depleted mitochondria from tafazzin knockdown heart (1).*

Aims

Cardiolipin is essential for multiple biological systems and pathways in mitochondria:

- ATP synthesis and energy conversion;
- Localization and interaction of mitochondrial enzymes;
- Apoptosis;
- Respiratory chain and assembly of Electron transport chain supercomplexes;
- Mitochondrial protein transport and recycling;
- Transport of metabolites across mitochondrial membranes;
- Maintenance of mitochondrial architecture;
- Mitochondrial fission and fusion.

Tafazzin knockdown mice develop dilated cardiomyopathy by 7-8 months of age (2).

We investigated the underlying mechanisms causing dilated cardiomyopathy in our mouse model of Barth syndrome and the impact of cardiolipin deficiency on mitochondrial proteomics and global gene expression patterns in cardiac cells.

Methods

We were interested in changes in the mitochondrial proteome and global gene expression patterns in 3-4 months old mice, an age prior to development of the cardiac phenotype.

Proteomics studies: Mitochondria were isolated from ventricular muscles of 3-months old WT and Taz-KD mice. We employed two-dimensional difference gel electrophoresis (**2D-DIGE**) to examine changes in mitochondrial proteomic landscape caused by cardiolipin deficiency in Taz-KD mouse heart with MS-based identification of differently represented proteins.

Gene Expression analysis: RNA samples were isolated from ventricular muscles of WT and Taz-KD mice. Global gene expression pattern was analyzed with an Affymetrix GeneChip Mouse oligonucleotide microarray.

Results

Combining proteomic and transcriptomic approaches with subsequent validation of results allows comprehensive assessment of pathological and compensatory changes in metabolic pathways in cardiolipin-deficient cardiomyocytes.

Proteomics studies: A total more than 2100 individual polypeptide spots were detected on each 2D gel, and the relative abundance of 82 polypeptides was significantly altered between control and Taz-KD groups. We selected 33 spots whose relative abundance was at least 1.5 fold different between WT and Taz-KD groups and subjected each to in-gel digestion and identification by MALD-TOF and TOF/TOF analyses.

Of 33 identifiable spots picked from 2-D gels, 22 corresponded to non-redundant mitochondrial protein sequences. Relative abundances of 14 spots were decreased in Taz-KD group *vs* controls. Among them were 8 polypeptides involved in assembly of respiratory chain complexes and CoQ10 biosynthesis. Mitochondria-bound myoglobin was also significantly reduced in CL-depleted mitochondria (Figure 2).

Relative abundances of other 8 polypeptides were increased in the Taz-KD group, perhaps reflecting adaptive remodeling of metabolic systems in cardiolipin-depleted cardiac mitochondria. Among them were enzymes involved in metabolism of amino acids, lipids, pyruvate and folate metabolism (Table 1).

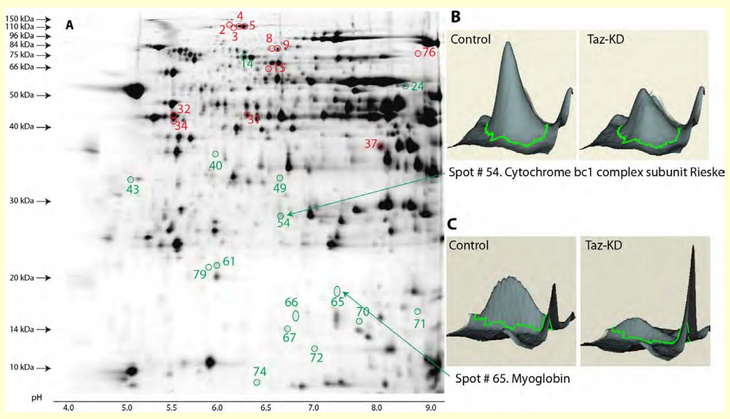

Figure 2. A – Representative 2D-gel of cardiac mitochondria. Circles indicate polypeptides relative abundance of which change at least 1.5 times in CL-depleted mitochondria vs controls (increased – green, decreased – red). B and C – Spots enclosed in green demonstrate the difference in volume of Rieske protein (B) and myoglobin (C) in WT and Taz-KD mitochondria.

Table 1. Changes in mitochondrial proteome in Taz-KD hearts.

Spot number	Top Ranked Protein Name (Species)	Accession No.	Total Ion C. I. %	Gel 1, KD / WT	Gel 2, KD / WT	Biological Pathway
	Increased in Taz-KD mitochondria					
5	Lon protease homolog, mitochondrial	LONM_MOUSE	100	2.8	3.1	ATP-dependent mitochondrial protease.
4			100	2.12	2.69	
76	Calcium-binding mitochondrial carrier protein Aralar2	CMC2_MOUSE	100	2.8	1.32	Ca2+-dependent mitochondrial aspartate/glutamate carrier.
37	Bifunctional methylenetetrahydrofolate dehydrogenase	MTDC_MOUSE	100	2.77	2.75	Folate / One carbon metabolism.
3	10-formyltetrahydrofolate dehydrogenase, Mitochondrial	AL1L2_MOUSE	100	2.69	2.5	Folate / One carbon metabolism.
2			100	2.46	2.15	
31	Acyl-coenzyme A thioesterase 2, mitochondrial	ACOT2_MOUSE	100	2.03	1.88	Metabolism of Acyl-CoAs, bile CoAs, and CoA esters of prostaglandins, to free acid and CoA.
34	Succinyl-CoA ligase [GDP-forming] subunit beta, mitochondrial	SUCB2_MOUSE	100	1.92	2.01	Pyruvate metabolism and TCA cycle.
32			100	1.84	1.73	
8	Delta-1-pyrroline-5-carboxylate synthase	P5CS_MOUSE	100	1.68	2.01	Amino acid synthesis and interconversion (transamination).
9			100	1.51	2.71	
15	Mitochondrial inner membrane protein	IMMT_MOUSE	100	1.83	1.42	Cristae junction and morpholgy. Component of MINOS complex.
	Decreased in Taz-KD mitochondria					
54	Cytochrome b-c1 complex subunit Rieske, mitochondrial	UCRI_MOUSE	100	-1.63	-1.57	Oxidative Phosphorylation. Complex III. Fe-S Protein.
49	Cytochrome c1, heme protein, mitochondrial	CYC1_MOUSE	100	-1.52	-1.47	Oxidative Phosphorylation. Complex III. Heme Protein.
74	NADH dehydrogenase alpha subcomplex subunit 5	NDUFA5_MOUSE	100	-1.54	-1.54	Oxidative Phosphorylation. Complex I, Fe-S Protein.
14	Succinate dehydrogenase flavoprotein subunit, mitochondrial	DHSA_MOUSE	100	-1.54	-1.64	Oxidative Phosphorylation. Complex II.
24	ATP synthase subunit alpha, mitochondrial	ATPA_MOUSE	100	-1.73	-1.76	Oxidative Phosphorylation. Complex V.
72	Iron-sulfur cluster assembly enzyme ISCU, mitochondrial	ISCU_MOUSE	100	-1.72	-1.67	Oxidative Phosphorylation. Assembly of Fe-S Scaffold proteins. MIM:255125
79	Ubiquinone biosynthesis protein COQ7 homolog	COQ7_MOUSE	100	-1.76	-1.71	Oxidative Phosphorylation. Ubiquinone biosynthesis.
43	Ubiquinone biosynthesis protein COQ9, mitochondrial	COQ9_MOUSE	100	-1.67	-1.57	Oxidative Phosphorylation. Ubiquinone biosynthesis.
71	Peptidyl-prolyl cis-trans isomerase F, mitochondrial	PPIF_MOUSE	100	-1.8	-1.49	Cyclophilin D: PTP modulator.
65	Myoglobin	MYG_MOUSE	100	-1.64	-2.41	Intracellular Oxygen Transport. Heart developmet in zebrafish.
66			100	-1.49	-2.14	
68			100	-1.41	-1.46	
61	Succinyl-CoA:3-ketoacid-coenzyme A transferase 1, mitochondrial	SCOT1_MOUSE	100	-1.79	-1.78	Key enzyme for ketone body catabolism. OMIM 245050.
40	Hexaprenyldihydroxybenzoate methyltransferase, mitochondrial	COQ3_MOUSE	96.938	-1.91	-1.74	Ubiquinone biosynthesis. Binding partner of Coq7.
67	Methylmalonyl-CoA epimerase, mitochondrial	MCEE_MOUSE	100	-1.5	-1.78	Degradation of branched chain amino acids and odd chain-length fatty acids.
70	Peroxiredoxin-5, mitochondrial	PRDX5_MOUSE	100	-1.59	-1.84	Prostaglandin 2 biosynthesis and metabolism FM.

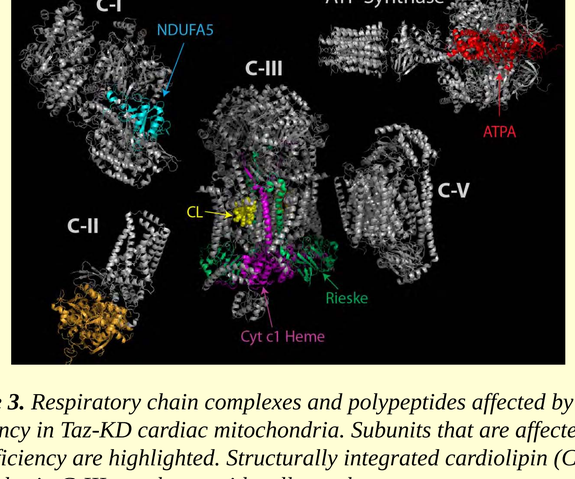

Figure 3. *Respiratory chain complexes and polypeptides affected by CL-deficiency in Taz-KD cardiac mitochondria. Subunits that are affected by CL-deficiency are highlighted. Structurally integrated cardiolipin (CL) molecules in C-III are shown with yellow spheres.*

Results *(continued)*

Gene expression analysis revealed significant downregulation of genes involved in muscle contraction, membrane trafficking, G-protein coupled receptor (GPCR) downstream signalling, axon guidance and others.

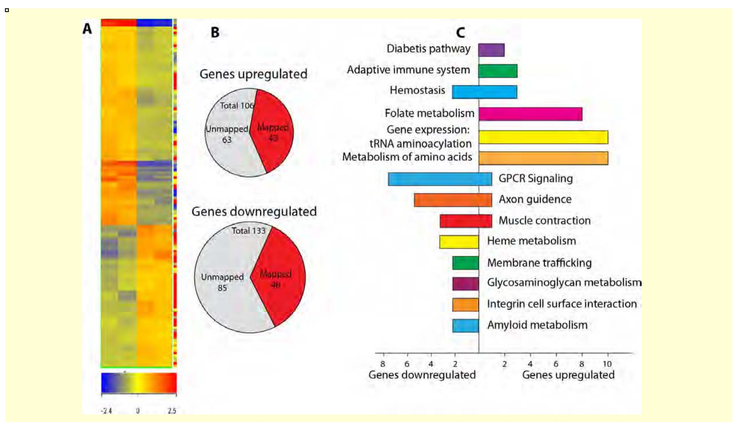

Figure 4. *A – Heat map depicting microarray-based profiling of gene expression in Taz-KD hearts. B – Global gene expression analysis revealed that 106 genes were upregulated and 113 were downregulated in Taz-KD hearts (cutoff ≥2.0). Genes that are mapped on biological pathways were identified with bioinformatics tools at www.reactome.org. Gene expression data were analyzed with GeneSpring GX software (Agilent Technologies). **C** – Chart shows functional classification of upregulated and downregulated mRNAs in Taz-KD mice. Each bar represents number of differently expressed genes from given pathway.*

Genes involved in one carbon / folate metabolism, amino acid metabolism and gene expression pathway were upregulated in Taz-KD hearts.

One of the most strongly induced mRNA in Taz-KD heart is musclin (*Ostn*). Musclin is small secreted hormone-like protein that is expressed in osteoblasts and fast glycolytic skeletal muscles. At the C-terminus, OSTN has homology with natriuretic peptides and interacts with type C natriuretic peptide receptor with high affinity. In skeletal muscle, OSTN inhibits activation of protein kinase B (AKT/PKB) in insulin signalling cascade. The significance of *Ostn* induction in cardiac muscle is unknown.

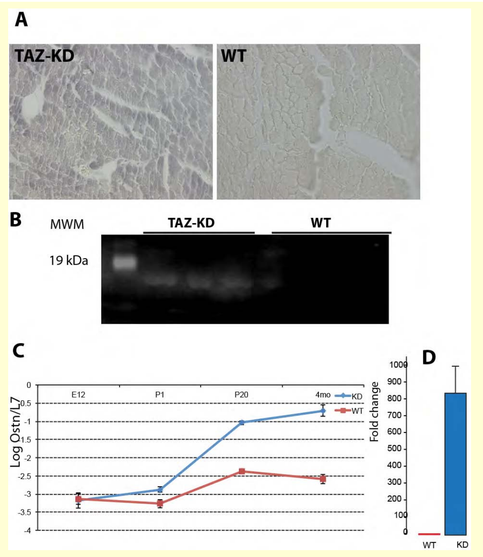

Figure 4. *Induction of of musclin (Ostn) expression in Taz-KD heart. **A** – Slides of cardiac ventricular muscle are stained with anti-musclin antibodies. **B** – Increased amount of circulating musclin in the blood of Taz-KD mice (western blot). **C** – Musclin expression in WT and Taz-KD mouse hearts at different stages of development (Graph on panel **C** is presented in logarithmic scale). At 4 months of age musclin expression in cardiac muscle of Taz-KD mice increased over 800-fold compared to WT controls (**D**).*

Summary:

- Relative abundance of subunits of mitochondrial respiratory chain complexes I, II, III and V are reduced in cardiolipin-deficient mitochondria of Taz-KD mouse heart.
- Mitochondrial-bound myoglobin is reduced in CL-deficient mitochondria.
- Musclin expression is dramatically induced in hearts of Taz-KD mice. The significance of musclin induction in cardiac muscle is unknown

Diminished activities of oxidative phosphorylation complexes in combination with reduced oxygen supply could be major pathogenic factors in development of cardiac phenotype in Taz-KD mice and BTHS patients.

1. Powers C, Huang Y, Strauss A, Khuchua Z. Diminished exercise capacity and mitochondrial bc1 complex deficiency in tafazzin knockdown mice. Frontiers in Physiology (2013) 4: 1.
2. Acehan D, Vaz F, Houtkooper R et al. Cardiac and skeletal muscle defects in a mouse model of human Barth syndrome. J Biol Chem (2011) 286 (2): 899.

Work is supported by Cincinnati Children's Research Foundation and NIH (RO1HL108867, ZK)